Magnetoelectric coupling and the manipulation of magnetic Bloch skyrmions

Zidong Wang, Zhao Ma, and Malcolm J. Grimson

Citation: Appl. Phys. Lett. **113**, 102403 (2018); doi: 10.1063/1.5049832
View online: https://doi.org/10.1063/1.5049832
View Table of Contents: http://aip.scitation.org/toc/apl/113/10
Published by the American Institute of Physics

Magnetoelectric coupling and the manipulation of magnetic Bloch skyrmions

Zidong Wang,[1,a)] Zhao Ma,[2] and Malcolm J. Grimson[3,a)]
[1]*State Key Laboratory of Low-Dimensional Quantum Physics and Department of Physics, Tsinghua University, Beijing 10084, China*
[2]*Department of Mechanical Engineering, The University of Western Australia, Perth 6009, Australia*
[3]*Department of Physics, The University of Auckland, Auckland 1010, New Zealand*

(Received 25 July 2018; accepted 20 August 2018; published online 5 September 2018)

Chiral-magnetic/ferroelectric composite systems offer the possibility of electrically inducing magnetic Bloch skyrmions [Wang and Grimson, Phys. Rev. B **94**, 014311 (2016)]. They are appealing for potential applications in spintronics due to their self-protection behavior. To realize skyrmion-based spintronic devices, it is essential to control the motions of the skyrmions. In this work, we propose a mechanical technique to manipulate skyrmions collinearly with a mobile external electric field that is imposed on the chiral-magnetic/ferroelectric system. The role of propagation velocity strongly impacts on the quality of magnetic skyrmions. *Published by AIP Publishing.*
https://doi.org/10.1063/1.5049832

Magnetic Bloch skyrmions are topological vortex-like spin structures with a range of sizes from 10 nm to approximately 100 nm, which have been introduced theoretically[1,2] and observed experimentally[3] in many studies. The existence of these skyrmions has been detected in chiral-magnetic (CM) crystals, such as the B20 metallic MnSi,[3] FeGe,[4] MnGe,[5] Mn-Fe-Ge alloys,[5] Fe-Co-Si alloys,[6] and the multiferroic Cu_2OSeO_3,[7,8] which has no inversion symmetry. This can allow the emergence of magnetic skyrmions due to their non-centrosymmetric lattice structure which gives rise to a Dzyaloshinskii-Moriya (asymmetric exchange) interaction (DMI).[1] In micromagnetics, this phenomenon is caused by the interplay of a weak nearest-neighbor collinear exchange interaction and the inherent Dzyaloshinskii-Moriya coplanar interaction. The competition between the two stabilizes the helicity of magnetic skyrmions.[2]

Lately, magnetic skyrmions attract much attention within the spintronics community for a possible application in memory devices and computing.[9] The inherent stability of these topologically protected structures combined with their low pinning probability to defects are intriguing characteristics. To use skyrmions as information holders, it is necessary to control their motion. Previous studies revealed several non-mechanical methods, such as by using electric currents,[10] spin-polarized currents,[11] microwave fields,[12] temperature gradients,[13,14] and magnons.[15] However, a mechanical method has not been explored. In this work, we investigate a mechanical technique to move magnetic Bloch skyrmions collinearly with a mobile electric field source.

Multiferroism allows us to create magnetic skyrmions by the electric polarization.[16–18] This is a result of the small magnetoelectric (ME) coupling between the magnetization and electric polarization fields. Unfortunately, the multiferroic insulators, e.g., Cu_2OSeO_3, have a low transition temperature and a limited magnetic response, which is adverse for applications.[19] But in composite systems, which are synthetic heterostructures of magnetic and ferroelectric (FE) orders can produce a remarkable ME coupling due to the microscopic mechanism of the strain-stress effect.[20] Specifically, a mechanical strain can be internally generated by applying an electric field in the FE film due to the piezoelectric effect, then this strain acts on the coupled CM film and results in a net magnetization due to the inverse magnetostrictive effect, as shown in Fig. 1. It is known as the converse ME effect.[21] A previous study has demonstrated that creation of skyrmions can be induced by the converse ME effect in a composite system that consists of a coupled CM and FE bilayer film.[18]

In a composite CM/FE bilayer, the magnetic skyrmions are moved by an external electric field source along the bilayer film as shown in Fig. 2(a) (Multimedia view). The CM film is on the top of the bilayer and it is glued to a FE film by a strong ME coupling. The CM film can support magnetic skyrmions. A localized electric field source is located above and below the bilayer. It can travel in a plane parallel to the film. Then, we carry out a spin dynamics method to determine the time dependent behaviors of the magnetic and electrical responses.

The magnetic component of the system having a CM structure is described by the classical Heisenberg model on a

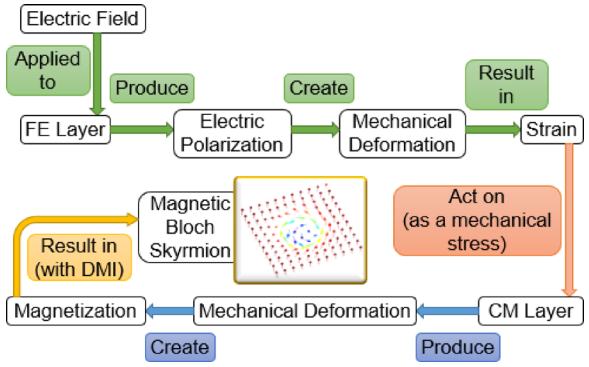

FIG. 1. The physical mechanism of the converse ME effect that forms magnetic Bloch skyrmions in the composite system. The processes of the reverse piezoelectric effect and inverse magnetostrictive effect are represented in the green and blue, respectively.

[a)]Authors to whom correspondence should be addressed: wangzidong@tsinghua.edu.cn and m.grimson@auckland.ac.nz

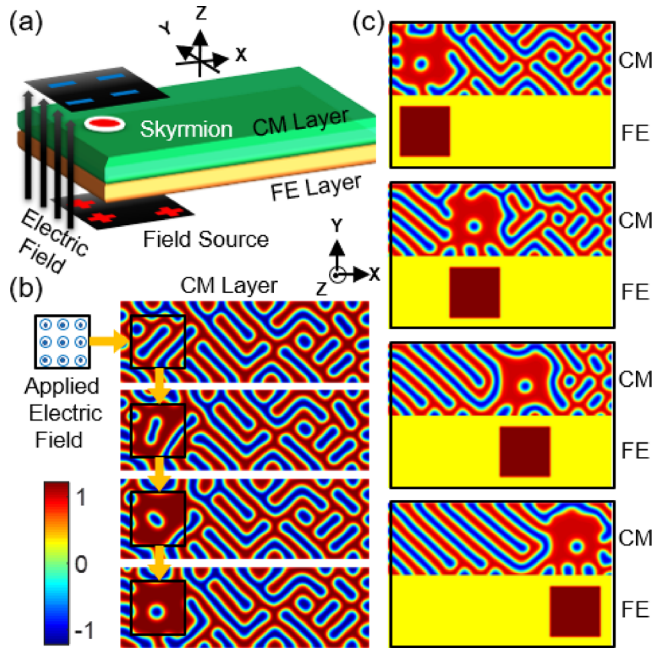

FIG. 2. (a) A schematic illustration of a composite bilayer consisting of a CM layer and a FE layer stacked at the interface. A localized electric field source can be moved longitudinally along the bilayer. (b) Sequential snapshots present the generation of a skyrmion in the bulk of the CM layer, as the localized electric field is statically applied at the initial position. (c) Propagating a skyrmion by moving the electric field source with a velocity of $v^* = 0.02$ spin-site/step. The color scale represents the magnitudes of the local z component magnetization and polarization. Multimedia views: https://doi.org/10.1063/1.5049832.1; https://doi.org/10.1063/1.5049832.2

two-dimensional rectangular lattice. The magnetic spin $\underline{S}_{i,j} = \left(S^x_{i,j}, S^y_{i,j}, S^z_{i,j}\right)$ characterizes the local magnetic moments, and it has a normalized length with $\|\underline{S}_{i,j}\| = 1$, and i,j locates the position. The total Hamiltonian $\mathcal{H}_{\mathrm{CM}}$ is given by

$$\begin{aligned}\mathcal{H}_{\mathrm{CM}} = &-J_{\mathrm{CM}} \sum_{i,j} [\underline{S}_{i,j} \cdot (\underline{S}_{i+1,j} + \underline{S}_{i,j+1})] \\ &- D \sum_{i,j} [(\underline{S}_{i,j} \times \underline{S}_{i+1,j})\hat{x} + (\underline{S}_{i,j} \times \underline{S}_{i,j+1})\hat{y}] \\ &- K \sum_{i,j} \left(S^z_{i,j}\right)^2 . \end{aligned} \tag{1}$$

The first term contains the familiar collinear nearest-neighbor exchange interaction, and $J^*_{\mathrm{CM}} = J_{\mathrm{CM}}/k_B T$ represents the dimensionless exchange interaction coupling coefficient. The second term shows the coplanar DMI in the two-dimensional lattice system, and $D^* = D/k_B T$ represents the dimensionless DMI coefficient, where $\hat{x}$ and $\hat{y}$ are the unit vectors along the x- and y-axes, respectively. This describes the Bloch-type DMI in a non-centrosymmetric crystal.[22] The third term represents the perpendicular magnetic anisotropy, and $K^* = K/k_B T$ is the dimensionless uniaxial anisotropic coefficient. The dynamics of magnetic spins have been studied by the well-known Landau-Lifshitz-Gilbert equation, which numerically solves the rotation of a magnetic spin in response to its torques

$$\frac{\partial \underline{S}_{i,j}}{\partial t} = -\gamma\left(\underline{S}_{i,j} \times \underline{H}^{\mathrm{eff}}_{i,j}\right) - \lambda_{\mathrm{CM}}\left[\underline{S}_{i,j} \times \left(\underline{S}_{i,j} \times \underline{H}^{\mathrm{eff}}_{i,j}\right)\right], \tag{2}$$

where γ is the gyromagnetic ratio which relates the spin to its angular momentum, and λ_{CM} is the phenomenological Gilbert damping term of CM materials.[23,24] $\underline{H}^{\mathrm{eff}}_{i,j} = -\delta\mathcal{H}/\delta\underline{S}_{i,j}$ is the effective field acting on each magnetic spin, which is the functional derivative of the system Hamiltonian.

We employ a pseudospin model to solve the dynamical behaviors of electric polarization.[25,26] The local electric moments are replaced by electric pseudospins, shown as $\underline{P}_{k,l} = \left(P^x_{k,l}, P^y_{k,l}, P^z_{k,l}\right)$ that is regarded as a continuous vector, and k,l characterizes the location. The distinction between pseudospins and classical spins is the variable size and absence of precession. The electric polarization is defined as the dipole moment density in dielectric materials. The dipole moment density p is proportional to the external electric field, , as $p = \epsilon_0 \chi_e E_{\mathrm{ext}}$. In the pseudospin model, the size of each electric pseudospin is proportional to the magnitude of its effective field as $\|\underline{E}^{eff}_{k,l}\| = \|\delta\mathcal{H}/\delta\underline{P}_{k,l}\|$. Hence $\|\underline{P}_{k,l}\| = \epsilon_0 \Xi_e \|\underline{E}^{eff}_{k,l}\|$, where Ξ_e is the dimensionless pseudoscalar susceptibility. Consequently, the electric pseudospin has a variable size as does the behavior of an electric dipole. We use a transverse Ising model to describe the Hamiltonian of pseudospins,[27] as

$$\begin{aligned}\mathcal{H}_{\mathrm{FE}} = &-J_{\mathrm{FE}} \sum_{i,j} \left[P^z_{k,l}\left(P^z_{k+1,l} + P^z_{k,l+1}\right)\right] \\ &-\Omega \sum_{i,j} \left(P^x_{k,l}\right) - \epsilon_0 \chi_e E_{\mathrm{ext}} \sum_{i,j} \left(P^z_{\tilde{k},\tilde{l}}\right), \end{aligned} \tag{3}$$

where $J^*_{\mathrm{FE}} = J_{\mathrm{FE}}/k_B T$ represents the dimensionless electric exchange coupling along the Ising z direction. $\Omega^* = \Omega/k_B T$ represents the dimensionless transverse field along the x axis, which is an in-plane field and perpendicular to the Ising z direction. $E^*_{\mathrm{ext}} = \epsilon_0 \chi_e E_{\mathrm{ext}}/k_B T$ represents the dimensionless applied electric field along the z direction, where ϵ_0 is the electric permittivity of free space, and χ_e is the dielectric susceptibility. A site of location $\tilde{k},\tilde{l}$ presents the pseudospin which in the presence of electric field. Note that the applied electric field is mobile, localized, and located to relative bilayer film to reduce edge effects (i.e., edge-merons) in the simulations.[28] The time evolution of pseudospins is expected to perform a precession free trajectory.[26] Because of the electric dipole moment is a measure of the separation of positive and negative charges along the Ising z direction. It is a scalar. Therefore, only the z component of pseudospin represents the real polarization. A modified Landau-Lifshitz-Gilbert equation is used to describe the pseudospin dynamics, as

$$\frac{\partial \underline{P}_{k,l}}{\partial t} = -\lambda_{\mathrm{FE}}\left[\underline{P}_{k,l} \times \left(\underline{P}_{k,l} \times \underline{E}^{\mathrm{eff}}_{k,l}\right)\right], \tag{4}$$

where λ_{FE} is the phenomenological damping term in the FE structure.

The interfacial effects between the CM and FE layers are caused by a ME coupling. The analytic expression for ME effect can be bilinear or nonlinear, particularly with respect to the thermal effect.[29] In this paper, we only account for low-energy excitations between the CM and FE layers and so we restrict ourselves to the bilinear expression of ME interaction, as

$$\mathcal{H}_{\mathrm{ME}} = -g \sum_{(i,j)(k,l)} \left(S^z_{i,j} P^z_{k,l}\right), \tag{5}$$

where $g^* = g/k_B T$ represents the dimensionless strength of the ME coupling. Nonlinear forms have not been studied here for simplicity and due to their minor effects in the micromagnetic modelling.

To investigate the dynamical manipulation of magnetic Bloch skyrmions, we implement dimensionless parameters $J^*_{\mathrm{CM}} = D^* = 1$, $K^* = 0.1$, $J^*_{\mathrm{FE}} = 0.8$, $\Omega^* = 0.1$, $g^* = 0.4$, $\gamma^* = 1$, and $\lambda^*_{\mathrm{CM}} = \lambda^*_{\mathrm{FE}} = 0.1$. Note that "$*$" characterizes dimensionless quantity. The number of magnetic spins and electric pseudospins was set to $N = 30 \times 90$ in each layer. Free boundary conditions and a random initial state were applied. Landau-Lifshitz-Gilbert equations are solved by a fourth-order Range-Kutta method. A marginal electric field was applied to order the FE and CM domain walls, and then we apply the localized electric field with a dimensionless magnitude of $E^*_{\mathrm{ext}} = 10$ perpendicular to the bilayer surface. The electric pseudospins quickly complete realignment, but the responses of magnetic spins have a delay. The generation process of a magnetic skyrmion in the bulk of the CM layer is summarized in Fig. 2(b). Subsequently, this field source is moved along the bilayer with a constant velocity. The velocity is measured as $v^* = \Delta N/\Delta t^*$, where ΔN corresponds to spatial movement to equivalent locations (i.e., spin-sites), and Δt^* is a dimensionless time step. Figure 2(c) shows a series of diagrams that show the skyrmion transport in the CM layer (Multimedia view). The skyrmions follow the polarized pseudospins in the FE layer for a velocity of $v^* = 0.02$ spin-site/step.

In this propagation process, we can see the skyrmion track deflecting to the bottom edge due to the skyrmion Hall effect.[30] The behavior of a skyrmion is topologically like a spinning disk and it generates a Magnus force when traveling longitudinally. So, it induces a transverse force during the translational motion of the skyrmion. The figure further shows the electric polarization reflecting the passage of field source. But the magnetization has a component that is non-collinear with the electric response and shows a spin spiral alignment due to the existence of a finite DMI. CM crystals have a non-centrosymmetric structure that enables the magnetic ordering to be broken.

The movement of the field source is externally controllable. We therefore explored two results of the effects of higher velocity on the skyrmion transport. Figure 3(a) shows a trial with a propagation velocity of $v^* = 0.05$ spin-site/step (Multimedia view). The skyrmion barely struggles to follow the motion of field source during the propagation process. Eventually, the system becomes more complicated, because another two skyrmions are formed from edge-merons to complement the energy contribution. In Fig. 3(b), we set the velocity to $v^* = 0.1$ spin-site/step and note the skyrmions are lost immediately (Multimedia view). Furthermore, the skyrmion Hall effect acts in the high-speed operation and the transverse motion of skyrmion transport may result in its annihilation at the boundaries.

The magnetization processes in the CM bilayer are consistent with the magnetic phase diagrams calculated earlier.[31,32] Furthermore the physics of isolated chiral skyrmions have been investigated[33] and they show that the formation of isolated skyrmions, their structure, and stability limits are consistent with the results shown here.

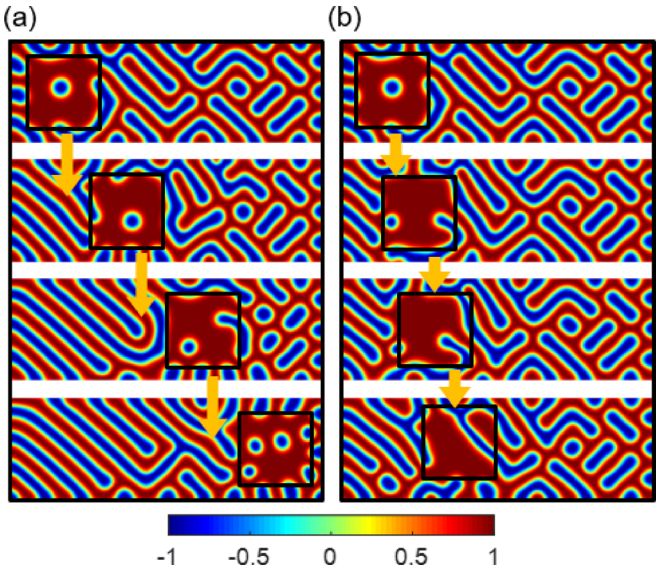

FIG. 3. High velocity effects on skyrmion transport for (a) $v^* = 0.05$ spin-site/step and (b) $v^* = 0.1$ spin-site/step. The color scale represents the magnitude of the z component magnetization. Multimedia views: https://doi.org/10.1063/1.5049832.3; https://doi.org/10.1063/1.5049832.4

In summary, we have investigated a mechanical method to control magnetic Bloch skyrmions by moving an electric field source parallel to the composite CM/FE bilayer system. Skyrmions are supported by the electric polarization through the converse ME effect. The results demonstrate that the skyrmion is moved collinearly with the field source at a slow speed. But higher speeds may break the stability of skyrmion transport and lead to annihilation of the skyrmions at the edges.

We would like to thank Xichao Zhang, Yan Zhou, and Wanjun Jiang for the discussion. Z.M. gratefully acknowledges Bingjing Zhao and Yuhua Wang for support.

[1]U. K. Rößler, A. N. Bogdanov, and C. Pfleiderer, Nature **442**, 797 (2006).
[2]N. Nagaosa and Y. Tokura, Nat. Nanotechnol. **8**, 899 (2013).
[3]S. Mühlbauer, B. Binz, F. Jonietz, C. Pfleiderer, A. Rosch, A. Neubauer, R. Georgii, and P. Böni, Science **323**, 915 (2009).
[4]X. Z. Yu, N. Kanazawa, Y. Onose, K. Kimoto, W. Z. Zhang, S. Ishiwata, Y. Matsui, and Y. Tokura, Nat. Mater. **10**, 106 (2011).
[5]K. Shibata, X. Z. Yu, T. Hara, D. Morikawa, N. Kanazawa, K. Kimoto, S. Ishiwata, Y. Matsui, and Y. Tokura, Nat. Nanotechnol. **8**, 723 (2013).
[6]W. Münzer, A. Neubauer, T. Adams, S. Mühlbauer, C. Franz, F. Jonietz, R. Georgii, P. Böni, B. Pedersen, M. Schmidt *et al.*, Phys. Rev. B **81**, 041203 (2010).
[7]S. Seki, X. Z. Yu, S. Ishiwata, and Y. Tokura, Science **336**, 198 (2012).
[8]T. Adams, A. Chacon, M. Wagner, A. Bauer, G. Brandl, B. Pedersen, H. Berger, P. Lemmens, and C. Pfleiderer, Phys. Rev. Lett. **108**, 237204 (2012).
[9]X. Zhang, M. Ezawa, and Y. Zhou, Sci. Rep. **5**, 9400 (2015).
[10]S. Woo, K. Litzius, B. Krüger, M. Y. Im, L. Caretta, K. Richter, M. Mann, A. Krone, R. M. Reeve, M. Weigand *et al.*, Nat. Mater. **15**, 501 (2016).
[11]A. Fert, V. Cros, and J. Sampaio, Nat. Nanotechnol. **8**, 152 (2013).
[12]S. K. Kim, O. Tchernyshyov, and Y. Tserkovnyak, Phys. Rev. B **92**, 020402(R) (2015).
[13]L. Kong and J. Zang, Phys. Rev. Lett. **111**, 067203 (2013).
[14]S. Lin, C. D. Batista, C. Reichhardt, and A. Saxena, Phys. Rev. Lett. **112**, 187203 (2014).

[15]C. Schütte, J. Iwasaki, A. Rosch, and N. Nagaosa, Phys. Rev. B **90**, 174434 (2014).
[16]P. Chu, Y. L. Xie, Y. Zhang, J. P. Chen, D. P. Chen, Z. B. Yan, and J. M. Liu, Sci. Rep. **5**, 8318 (2015).
[17]M. Mochizuki and Y. Watanabe, Appl. Phys. Lett. **107**, 082409 (2015).
[18]Z. D. Wang and M. J. Grimson, Phys. Rev. B **94**, 014311 (2016).
[19]J. G. Bos, C. V. Colin, and T. T. M. Palstra, Phys. Rev. B **78**, 094416 (2008).
[20]C. W. Nan, Phys. Rev. B **50**, 6082 (1994).
[21]W. Eerenstein, N. D. Mathur, and J. F. Scott, Nature **442**, 759 (2006).
[22]W. Koshibae, Y. Kaneko1, J. Iwasaki, M. Kawasaki, Y. Tokura, and N. Nagaosa, Jpn. J. Appl. Phys. **54**, 053001 (2015).
[23]T. L. Gilbert, IEEE Trans. Magn. **40**, 3443 (2004).
[24]G. M. Wysin, *Magnetic Excitations and Geometric Confinement* (IOP Publishing, Bristol, 2015).
[25]Z. Wang and M. J. Grimson, J. Appl. Phys. **118**, 124109 (2015).
[26]Z. Wang and M. J. Grimson, J. Appl. Phys. **119**, 124105 (2016).
[27]C. L. Wang, S. R. P. Smith, and D. R. Tilley, J. Phys.: Condens. Matter **6**, 9633 (1994).
[28]J. Müller, A. Rosch, and M. Garst, New J. Phys. **18**, 065006 (2016).
[29]L. Chotorlishvili, S. R. Etesami, J. Berakdar, R. Khomeriki, and J. Ren, Phys. Rev. B **92**, 134424 (2015).
[30]W. Jiang, X. Zhang, G. Yu, W. Zhang, M. B. Jungfleisch, J. E. Pearson, O. Heinonen, K. L. Wang, Y. Zhou, A. Hoffmann, and S. G. E. te Velthuis, Nat. Phys. **13**, 162 (2017).
[31]A. B. Butenko, A. A. Leonov, U. K. Rößler, and A. N. Bogdanov, Phys. Rev. B **82**, 052403 (2010).
[32]M. N. Wilson, A. B. Butenko, A. N. Bogdanov, and T. L. Monchesky, Phys. Rev. B **98**, 094411 (2014).
[33]A. O. Leonov, T. L. Monchesky, N. Romming, A. Kubetzka, A. N. Bogdanov, and R. Wiesendanger, New J. Phys. **18**, 065003 (2016).